Astronomy & Astrophysics manuscript no. sn2008iz˙paper1
March 25, 2010

VLBI observations of SN 2008iz:

I. Expansion velocity and limits on anisotropic expansion

A. Brunthaler[1], I. Martí-Vidal[1], K.M. Menten[1], M.J. Reid[2], C. Henkel[1], G.C. Bower[3], H. Falcke[4,5], H. Feng[6], P. Kaaret[7], N.R. Butler[3], A.N. Morgan[3], and A. Weiß[1]

[1] Max-Planck-Institut für Radioastronomie, Auf dem Hügel 69, 53121 Bonn, Germany
e-mail: brunthal@mpifr-bonn.mpg.de
[2] Harvard-Smithsonian Center for Astrophysics, 60 Garden Street, Cambridge, MA 02138, USA
[3] UC Berkeley, 601 Campbell Hall, Astronomy Department & Radio Astronomy Lab, Berkeley, CA 94720, USA
[4] Department of Astrophysics, Radboud Universiteit Nijmegen, Postbus 9010, 6500 GL Nijmegen, the Netherlands
[5] ASTRON, Postbus 2, 7990 AA Dwingeloo, the Netherlands
[6] Department of Engineering Physics and Center for Astrophysics, Tsinghua University, Beijing 100084, China
[7] Department of Physics and Astronomy, University of Iowa, Van Allen Hall, Iowa City, IA 52242, USA

Received

ABSTRACT

We present observations of the recently discovered supernova 2008iz in M82 with the VLBI High Sensitivity Array at 22 GHz, the Very Large Array at frequencies of 1.4, 4.8, 8.4, 22 and 43 GHz, and the Chandra X-ray observatory. The supernova was clearly detected on two VLBI images, separated by 11 months. The source shows a ring-like morphology and expands with a velocity of ∼ 23000 km s^{-1}. The most likely explosion date is in mid February 2008. The measured expansion speed is a factor of ∼2 higher than expected under the assumption that synchrotron self-absorption dominates the light curve at the peak, indicating that this absorption mechanism may not be important for the radio emission. We find no evidence for an asymmetric explosion. The VLA spectrum shows a broken power law, indicating that the source was still optically thick at 1.4 GHz in April 2009. Finally, we report upper limits on the X-ray emission from SN 2008iz and a second radio transient recently discovered by MERLIN observations.

Key words. (Stars:) supernovae: general, (Stars:) supernovae: individual: SN 2008iz, Radio continuum: general, Galaxies: individual: M82

1. Introduction

Radio supernovae (RSNe) are rare events and difficult to study. So far only about two dozen have been detected (e.g Weiler et al. 2002) and most of them are quite distant and rather weak. Only few radio supernovae have been imaged with Very Long Baseline Interferometry (VLBI) techniques and for only four has it been possible to study the evolution of the expanding shell (SN 1979C, SN 1986J, SN 1987A, SN 1993J). The best studied radio supernova so far is SN 1993J in M81. Following the expansion of the supernova allowed many different phenomena to be studied (Marcaide et al. 1997, 2009a; Bietenholz et al. 2001, 2003; Pérez-Torres et al. 2001, 2002a; Bartel et al. 2002, 2007), including a measurement of the expansion speed, the deceleration of the shock front, and the proper motion of the supernova shell, for which a limit was obtained.

The recent discovery of a new bright radio supernova in M82, SN 2008iz, (Brunthaler et al. 2009a,b) at a similar distance as SN 1993J offers the rare opportunity to study the evolution of another supernova in great detail and to make a comparison to SN 1993J. So far, SN 2008iz was only detected in the radio band, with the VLA at 22 GHz (Brunthaler et al. 2009a), MERLIN at 5 GHz (Beswick et al. 2009), and the Urumqi telescope at 5 GHz (Marchili et al. 2010). There are no reported detections in visible light and Fraser et al. (2009) report only a non detection in the near infrared on 2009 June 11. The non-detections at other wavebands indicate that the supernova exploded behind a large gas or dust cloud in the central part of M82. Thus, it has not been possible to classify this supernova. However, since type Ia supernovae are not known to show strong radio emission, SN 2008iz is most likely a core collapse supernova, i.e. type Ib/c or II.

Here we present the first VLBI images of SN 2008iz taken ∼2.5 and ∼13.5 month after the explosion, a radio spectrum (at an age of ∼14.5 month) from 1.4 to 43 GHz and Chandra X-ray observations. Throughout the paper, we adopt a distance of 3.6 Mpc (based on a Cepheid distance to M81 determined by Freedman et al. 1994).

2. Observations and data reduction

2.1. High Sensitivity Array observations at 22 GHz

M82 was observed using the High Sensitivity Array including the NRAO[1] Very Long Baseline Array (VLBA), the Very Large Array (VLA), the Green Bank Telescope (GBT), and the Effelsberg 100m telescope under project code BB255 on 2008 May 03 and 2009 April 08. The total observing time at each epoch was 12 hours. We used M81*, the nuclear radio source in M81, as phase calibrator and switched between M81*, M82, and 3 extragalactic background quasars every 50 seconds in the cycle M81* – 0945+6924 – M81* – 0948+6848 – M81* – M82

[1] The National Radio Astronomy Observatory is a facility of the National Science Foundation operated under cooperative agreement by Associated Universities, Inc.

– 1004+6936 – M81*, yielding an integration time of ∼100 minutes on M82. J1048+7143 was observed every ∼30 minutes to phase-up the VLA. Furthermore, DA193 was observed as fringe finder. The data were recorded with four 8 MHz frequency bands in dual circular polarization, with Nyquist sampling and 2 bits per sample (i.e., a total recording rate of 256 Mbit s^{-1}).

Before, in the middle, and at the end of the phase referencing observations, we included *geodetic blocks*, where we observed 18–21 bright sources from the International Celestial Reference Frame (ICRF) at 22 GHz for ∼75 minutes to measure the tropospheric zenith delay offsets at each antenna (for a detailed discussion see Reid & Brunthaler 2004; Brunthaler et al. 2005). The geodetic blocks were recorded with 8 IFs of 8 MHz in left circular polarization. The first IF was centered at a frequency of 22.01049 GHz, and the other seven IFs were separated by 12.5, 37.5, 100.0, 262.5, 312.5, 412.5, and 437.5 MHz, respectively. Here, only a single VLA antenna was used, which could observe only five IFs at 0.0, 12.5, 37.5, 412.5, and 437.5 MHz relative to 22.01049 GHz.

The data were correlated at the VLBA Array Operations Center in Socorro, New Mexico. In the observation on 2008 May 03, the data were correlated at the position of known water maser emission ($09^h55^m51^s.38702$, $+69°40'44''.4676$, J2000) with 128 spectral channels per IF and an integration time of 1 second. The observation on 2009 April 08 was correlated at the position $09^h55^m51^s.5500$, $+69°40'45''.792$, (J2000), close to SN 2008iz with 16 spectral channels and an integration time of 1 second.

The data reduction was performed with the NRAO Astronomical Image Processing System (AIPS) and involved standard steps. First we shifted the position of M82 to the position of SN 2008iz using CLCOR in the observation on 2008 May 03. We applied the latest values of the Earth's orientation parameters and performed zenith delay corrections based on the results of the geodetic-like observations. Total electron content maps of the ionosphere were used to correct for phase changes by the ionosphere. A-priori amplitude calibration was applied using system temperature measurements and standard gain curves. We performed a "manual phase-calibration" using the data from J1048+7143 to remove instrumental phase offsets among the frequency bands. Then, we fringe fitted the data from M81* and performed an amplitude self-calibration on M81*. In the observation on 2008 May 03, we also performed, first, a phase-self calibration and later an amplitude self-calibration on SN 2008iz. In the observation on 2009 April 08, the inclusion of the phased VLA increased the noise in the images significantly, possibly due to a problem with the phasing of the array (the VLA was in B-configuration). Thus, we flagged the VLA data from this epoch.

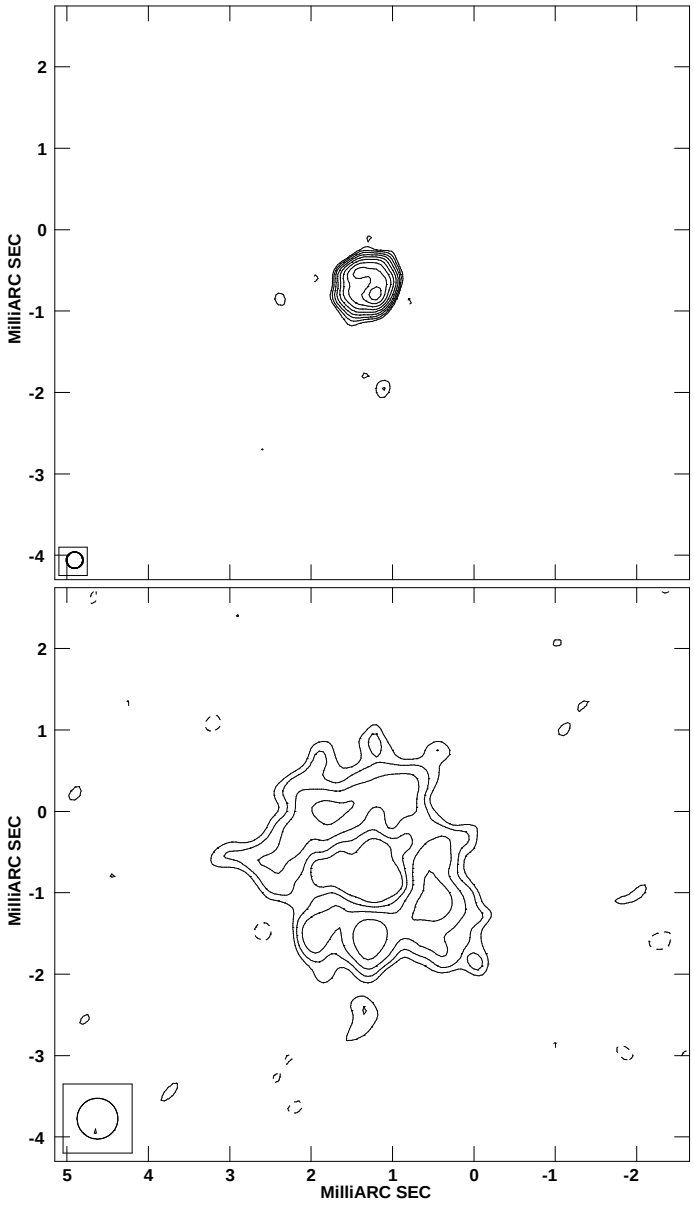

Fig. 1. HSA contour plots of SN 2008iz at 22 GHz in May 2008 (top) and April 2009 (bottom). Contours start at 0.3 mJy (top), 0.1 mJy (bottom) and increase with $\sqrt{2}$. The images are restored with a circular beam of FWHM 0.2 mas (top) and 0.5 mas (bottom). The original beam sizes were 0.31×0.23 mas at a position angle of −34° at the first epoch and 0.39×0.27 at a position angle of −40° at the second epoch.

2.2. VLA observation on 2009 April 27 (1.4-43 GHz)

We observed M82 with the VLA on 2009 April 27 at 1.4, 4.8, 8.4, 22, and 43 GHz. The total observing time was 4 hours. We observed with two frequency bands of 50 MHz, each in dual circular polarization. 3C 48 and J1048+7143 were used as primary flux density and phase calibrators, respectively. At 1.4, 4.8, and 8.4 GHz, we used a switching cycle of six minutes, spending one minute on the phase calibrator and five minutes on M82. We repeated these cycles 5 times over the observations, yielding an integration time of ∼25 minutes at each frequency. At 22 and 43 GHz, we used a switching cycle of three minutes, spending one minute on the phase calibrator and two minutes on M82. These cycles were repeated 10 times during the observation, yielding an integration time of ∼20 minutes at both frequencies.

The data reduction was performed in AIPS and involved amplitude calibration of 3C 48 using source models. Then we calibrated the phases using J1048+7143 and made one phase and amplitude self-calibration on J1048+7143. The calibration was then transferred to the target source M82. We performed one phase self-calibration on M82 at all frequencies except 43 GHz, where the source is too weak.

2.3. Chandra and Swift XRT observations

The Chandra X-ray observatory (CXO) observed M82 on 2008 October 4, and 2009 April 17 and 29. Each observation was taken with an exposure of about 18 ks. In these observations,

Table 1. Flux densities of SN 2008iz and two other supernova remnants in M82 from the VLA observation on 2009 April 27.

Source	$F_{1.4\,GHz}$ [mJy]	$F_{4.8\,GHz}$ [mJy]	$F_{8.4\,GHz}$ [mJy]	$F_{22\,GHz}$ [mJy]	$F_{43\,GHz}$ [mJy]
SN 2008iz	55.3±6.0	29.5±4.5	13.7±2.5	6.2±0.7	2.5±0.4
44.01+596	–	14.7±5.3	15.0±2.0	8.7±0.6	3.6±0.4
45.17+612	–	8.5±1.6	5.8±0.7	3.0±0.9	0.8±0.3

the target is off the optical axis by more than 3 arcmin, where the point spread function looks like an extended ellipse covering multiple pixels.

M82 was also observed with the Swift X-ray Telescope (XRT; Gehrels et al. 2004; Burrows et al. 2005) on 2007 January 26, 2008 May 1, and 2009 April 25 with exposures of 4.6 ks, 5.0 ks, and 4.7 ks, respectively. Due to the low resolution of the telescope, the collection of known X-ray sources looks point-like in the XRT data, so count rates from the conglomerate of sources were measured. The data suffer from heavy pile-up, which is accounted for by extracting count rates from an annular region around the central, piled-up location [2].

3. Results

3.1. VLBI images at 22 GHz

We imaged the data of SN 2008iz from 2008 May 03 with a slightly super-resolved beam of 0.2 × 0.2 mas. The peak flux density was 5.9 mJy beam^{-1}, the total emission was 32 mJy and we achieved an image rms of 79 μJy beam^{-1}. The data from 2009 April 08 were imaged with natural weighting and a circular beam of 0.5 × 0.5 mas to have more sensitivity for extended emission. Here, the peak flux density was 0.36 mJy beam^{-1}, the total emission was 4.3 mJy, and we achieved an image rms of 41 μJy beam^{-1}.

The supernova was clearly detected in both epochs (see Fig. 1). The source is already clearly resolved in the observation on 2008 May 03 and shows a ring like structure, typical for a radio supernova. In the following eleven months the source expanded and faded significantly.

3.2. VLA radio spectrum

M82 was imaged at all frequencies using only data from baselines larger than 30 kλ. This ensures that most of the extended emission in M82 is resolved out. Flux densities were extracted by fitting two-dimensional Gaussians to the images.

The measured flux densities of SN 2008iz and two other supernova remnants that could be easily separated from the diffuse background emission are listed in Table 1. The errors are estimated by adding in quadrature the formal error from the fit to the images, the difference between peak and integrated flux densities, and an 5% error allowing for an error in the overall flux density scale. Furthermore, we added an additional 5% error at 1.4, 4.8, and 8.4 GHz since we have more confusion from the extended emission at these frequencies. Note that the flux density at 4.8 GHz is in good agreement with the flux densities reported by Beswick et al. (2009), obtained with MERLIN a few days later (28.5± 2 mJy).

[2] Given the pile-up and uncertainty in the XRT astrometry on the order of a few arcseconds, attempting to separate any supernova flux from the other flux is practically impossible

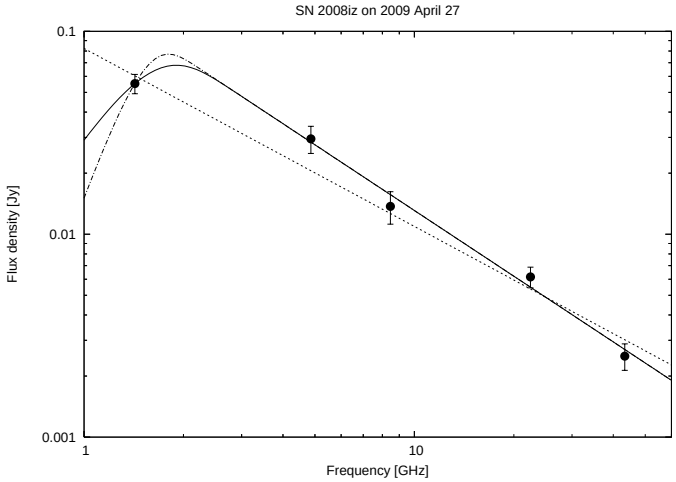

Fig. 2. Spectrum of SN 2008iz taken with the VLA on 2009 April 27. Also shown are a single power-law fit (dotted line) and two broken power-law fits with a spectral index of 2.5 (solid line) and 4.5 (dash-dotted line) in the optically thick part.

The spectrum of SN 2008iz is shown in Fig. 2. First, we fitted a single power-law spectrum to the data. This gives a spectral index of −0.88±0.07. However, the fit has a large reduced χ^2 value of 2.6, since the 1.4 GHz value is too low. Thus, we fitted the spectra also with a broken power-law,

$$S(\nu) = S_0 \left(\frac{\nu}{\nu_0}\right)^{\alpha} \left(1 - e^{-\left(\frac{\nu}{\nu_0}\right)^{\delta-\alpha}}\right), \quad (1)$$

where α and δ are the spectral indices of the optically thin and thick parts of the spectrum. S_0 and ν_0 represent the maximum flux density and the peak frequency of the fitted spectrum. Since one data point in the optically thick part of the spectrum is not enough to fit the spectral index there, we made two fits, one with a value for a synchrotron self-absorbed spectrum (δ =2.5), and a steeper free-free absorbed spectrum (δ=4.5). The reduced χ^2 values in both cases are now 0.9. The fit (using $\delta = 4.5$) gives a spectral index in the optically thin part of $\alpha = -1.08 \pm 0.08$ and a turnover frequency of $\nu_0 = 1.51 \pm 0.09$ GHz. While the spectral index α is not affected by the choice of δ, ν_0 changes slightly to 1.55 for $\delta = 2.5$. This indicates that the source was still optically thick, and brightening at the lowest frequencies in April 2009 (for comparision: SN 1993J reached it's peak at 1.4 GHz ∼500 days after the explosion; Weiler et al. 2002).

3.3. X-ray upper limits

The off-axis configuration and consequently the degraded angular resolution, as well as the diffuse background, have largely decreased the sensitivity of the Chandra measurements. The detection limit of these observations is estimated from the total emission around the radio position in a region with the same size as the point spread function. SN 2008iz is located close to several variable ultraluminous X-ray sources. However, no emission was detected at the position of the supernova. Muxlow et al. (2009) and Muxlow et al. (2010) report the discovery of a second radio transient in M82 with the MERLIN telescope. This source appeared between 2009 April 24 and 2009 May 5 and is located at a position with a diffuse emission background. It is surrounded by a few point-like sources. There is no enhanced X-

ray emission at the location of this second radio transient, neither on 2009 April 17, nor on 2009 April 29.

To compare our limits with the emission from SN 1993J, we assume spectral properties that are similar to the ones of SN 1993J at a similar age, i.e., a thermal bremsstrahlung spectrum with a temperature of 1.05 keV, abundances from Table 2, Column 4 of Zimmermann & Aschenbach (2003), and an absorption column density of 5.4×10^{22} cm^{-2} (see Sect. 5.1). Then we get an 3 σ upper limit of 1.5×10^{39} erg s^{-1} in the energy range 0.3-2.4 keV. This is consistent with the X-ray luminosity of SN 1993J at a similar age (Zimmermann & Aschenbach 2003) in the same energy range.

The 3 σ sensitivity at the location of the MERLIN transient, assuming a column density of 10^{22} cm^{-2} and a photon power-law index of 1.7 (an approximation to a thermal bremsstrahlung spectrum with a temperature of 10 keV, as seen in SN1995N; Fox et al. 2000), is found to be about 1.2×10^{38} erg s^{-1} in 0.3–2.4 keV, which we take as the upper limit of the X-ray luminosity.

The resultant count rates in the Swift XRT data (0.5-8.0 keV) are 0.60±0.02, 0.59±0.02, and 0.68±0.02 s^{-1} on 2007 January 26, 2008 May 1, and 2009 April 25, respectively. There is no clear rise in total flux from the pre-SNe observation to the May 2008 post-explosion epoch at ∼75 days, and while a ∼15% increase in count rate is seen in the final observation, this is consistent with BeppoSAX observations of the central region of M82 showing variations on the order of 15-30% (2-10 keV) on hour time-scales (Cappi et al. 1999). Indeed, such intrinsic variations are also seen over the course of each epoch in the XRT observations as well. Given the complications with the data and the intrinsic variability of the sources, strong constraints are difficult. However, since no increase in flux larger than the intrinsic variability is seen, we can place an upper limit on the SNe X-ray flux of approximately 1.5×10^{41} erg s^{-1} (0.5-2.4 keV) on 2008 May 1 (assuming the same model as for the Chandra observations above).

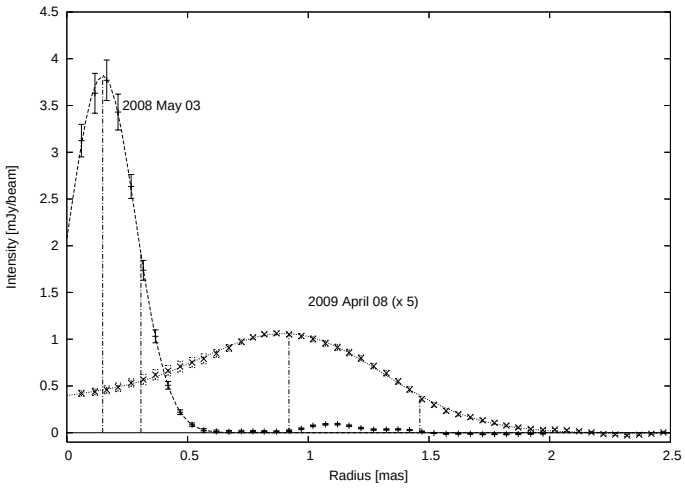

Fig. 3. Intensity of concentric rings of widths 0.05 mas in the images from 2008 May 03 and 2009 April 08. The flux densities in the second observation were scaled by a factor of 5. The vertical lines mark the position of the peak and the radius where the intensity is 50% of the peak level.

4. Expansion speed and explosion center

4.1. Estimates of size and position

Estimating a physical size from the VLBI data is not straightforward. Different methods have been applied to determine the expansion curves of several radio supernovae (e.g. Bartel et al. 2002; Marcaide et al. 2009a,b). Estimating the source size in the image plane may have *running biases* (i.e., biases that depend on the source size) related to the different resolutions achieved in the different images (i.e., the structure is better resolved as the source expands). One way to avoid such biases is to use a *dynamic beam*, i.e., a similar ratio between source size and beam size (e.g. Marcaide et al. 1997) at each epoch. Here we use several different methods to determine the source size. The results for each method are summarized in Table 2.

4.1.1. Concentric Rings

First, we have measured the intensity in concentric rings (of 0.05 mas width) using the AIPS task IRING. Examples of intensity profiles for both observations are shown in Fig. 3 together with fits to the data. One can define the radius $R_{n\%}$ where the intensity falls to n% of the peak intensity, with an arbitrary value for n. Since $R_{n\%}$ can be multi-valued (i.e., the inner and the outer radius), we always use the outer radius. Fig. 3 shows also the $R_{100\%}$ (i.e. the peak itself) and $R_{50\%}$ values. A value of n=50% has the advantage that the profile is much steeper and the position can be better determined than at the peak (where the profile is flat). In order to avoid a running bias, it is important to use in each epoch a similar ratio of source size to beam size (i.e. a dynamic beam). This method will give a size which is equal to the real size of the expanding shell times an unknown factor. This factor will be smaller for large values of n (the measured sizes are smaller for large values of n). Figure 4 shows the images of SN 2008iz at both epochs and an image of the second epoch with a dynamic beam together with the two $R_{50\%}$ source sizes.

It is important to note that the intensity profile is sensitive to the position of the central pixel of the concentric rings. A position offset would smear out the intensity profile. This can be seen in Fig. 5 where we plot the width of the intensity profile for different position offsets in the first observation. As expected, the width shows a strong dependence on the position offset, and the position of the center of the shell can be estimated. The position of the center is located in the first epoch at $09^h55^m51^s.55026$, $+69°40'45''.7913$ (J2000). The uncertainty in the absolute position is dominated by the uncertainty of the position of the phase referencing source M81* (∼0.5 mas).

4.1.2. Common Point Method

A different method that uses the concept of a dynamic beam in a natural way is the Common-Point Method (CPM, Marcaide et al. 2009a). This method relies on the existence of a point in the radial profile of the supernova structure that remains unaltered under small changes in the convolving beam. This point is closely related to the source size (indeed, the ratio between the radial position of this point and the source radius is ∼ 1; see Appendix A of Marcaide et al. 2009a, for details). In Fig. 6 we show the radial intensity profiles of SN 2008iz, computed from the azimuthal averages of the CLEAN models convolved using different beams. The "common points" in the profiles can be clearly seen in the figure.

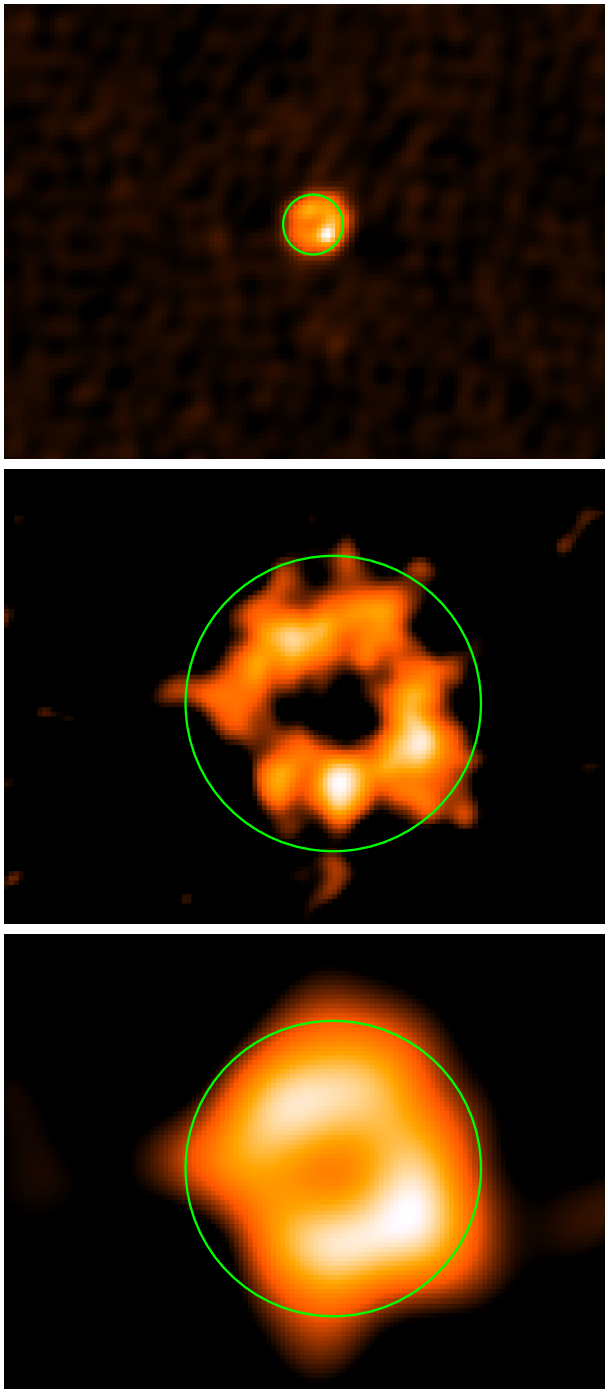

Fig. 4. HSA images at 22 GHz of SN 2008iz in May 2008 (top) and April 2009 (middle and bottom). The bottom image is convolved with a dynamic beam of 0.99 mas (i.e. the ratios of beam size and source size are identical in the top and bottom images). The rings denote the best fitted positions and radii from CPM in both epochs, i.e. 320 and 1580 μas.

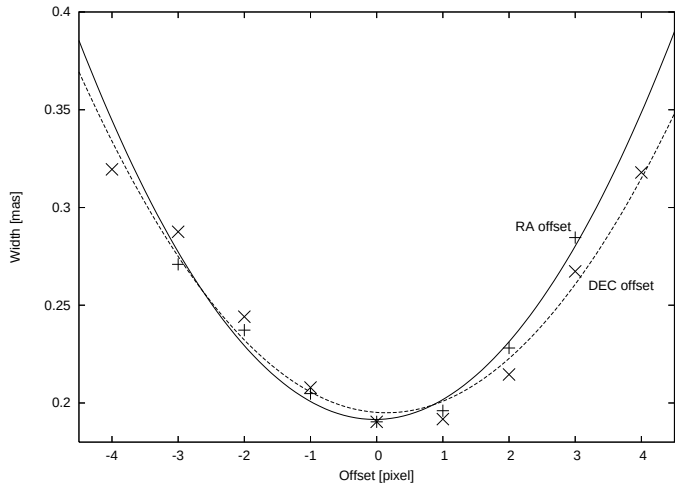

Fig. 5. The width of the intensity profile as a function of position offset (relative to a reference pixel) in the observation on 2008 May 03 One pixel corresponds to 0.05 mas. Shown are position offsets in right ascension (+) and declination (x).

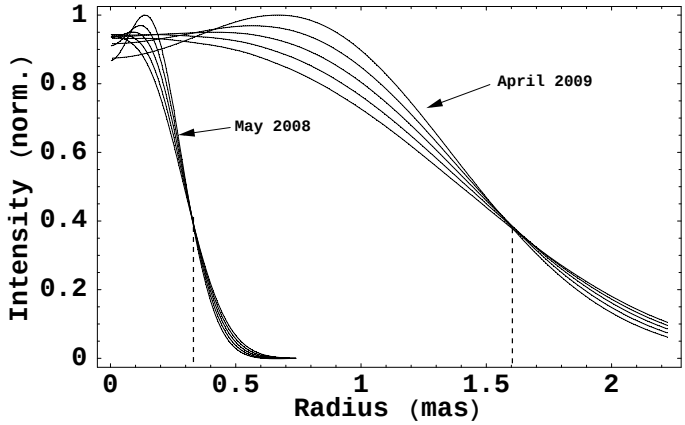

Fig. 6. Solid lines: radial intensity profiles of SN 2008iz at the two VLBI epochs, computed using different convolving beams (1.0, 1.1, 1.2, 1.3, and 1.4 times the source radius at each epoch). The radial positions of the common points at each epoch (see Section 4.1.2) are marked with dashed lines.

4.1.3. Model Fitting

Finally, we estimated the size from model-fitting to the visibilities, using a simplified model of the supernova radio structure. This method may have undetermined running biases if the model fitted to the visibilities is not a good representation of the true supernova emission structure. We fitted the visibilities using a model of a spherical shell of 30% fractional width. This is the model that best describes the structure of SN 1993J in Marcaide et al. (2009a). A smaller fractional width between 20 and 25%, as prefered by other authors (Bartel et al. 2000, 2002; Bietenholz et al. 2003) or predicted by Chevalier (1982), could lead to different source sizes. However, the current data, based only on two epochs at one frequency, do not allow a relaible statement about the true fractional width of SN2008iz. For the model-fitting, we used a modified version of the subroutine MODELFIT in the program DIFMAP (Shepherd et al. 1995), which fits a parameterized shell model to the real and imaginary parts of the visibilities. The use of the real and imaginary parts of the visibilities (instead of amplitudes and phases) is more robust from a statistical point of view, especially in the case of a low signal-to-noise ratio, since the noise involved in the data is gaussian-like (as assumed in the modelling algorithms based on a χ^2 minimization).

Table 2. Source sizes, expansion speeds, a lower limit for the expansion index *m*, and explosion dates (in 2008) assuming m=1 and m=0.89 for the different methods outlined in Section 4.1.

Method	R_{2008} [μas]	R_{2009} [μas]	$v_{exp,m=1}$ km s^{-1}	t_0 (m=1)	m	t_0 (m=0.89)
$R_{100\%}$	149	1008	15800	Mar 05	>0.86	Mar 19
$R_{50\%}$	307	1462	21200	Feb 02	>0.70	Feb 22
$R_{25\%}$	380	1676	23800	Jan 24	>0.66	Feb 14
CPM	320	1580	23100	Feb 07	>0.71	Feb 25
MODELFIT	320	1390	19600	Jan 22	>0.65	Feb 12

4.2. Expansion speed

Using the $R_{50\%}$ value as physical size, we get a radius of 307 μas on 2008 May 03 and 1462 μas on 2009 April 08. The measured sizes correspond to an average expansion speed of 1243 μas yr^{-1} or v_{exp}=21200 km s^{-1}. Extrapolating this expansion back to a radius of zero and assuming constant expansion ($r \propto t^m$ with an expansion index m=1) leads to an explosion date t_0 of 2008 February 02. However, a significant deceleration (i.e. $m < 1$) would shift the explosion date to a later time. Since the supernova was first seen in a VLA observation on 2008 March 24, one can use this to give a lower limit for the expansion index m of 0.7. Marchili et al. (2010) model the 5 GHz light curve of SN 2008iz and find evidence of a modest deceleration with an expansion index m=0.89 and an explosion date of 2008 February 18 (±6 days). Extrapolating the expansion seen on the VLBI images backward using this expansion index, yields an explosion date of 2008 February 22. This value for the explosion date is in reasonable agreement with the estimate from the 5 GHz light curve.

The resulting source sizes for the different methods are summarized in Table 2. Most methods give similar expansion speeds between 19600 and 23800 km s^{-1}. Since the $R_{100\%}$ values give a significantly lower expansion speed and a very late explosion date, we conclude that the $R_{100\%}$ values underestimate the true source sizes significantly. Hence, we do not consider these values for our further analysis. Based on the information of the two VLBI images, we thus conclude that the explosion occured between 2008 January 22 and 2008 March 24. We get a lower limit for the expansion index of m >0.65, and an average expansion speed in the range of 19600 – 23800 km s^{-1}.

Since the CPM source sizes should be very close to the real sizes, the expansion speed is very close to the average value of all methods (~22000 km s^{-1}, excluding $R_{100\%}$ which is clearly an outlier), and the explosion date is in very good agreement with the light curve modeling, we adopt these values. The formal errors in our various fits are exceedingly small (of the order of 20 μas). Since the systematic errors from the different methods are much larger, the spread in velocities (±1650 km s^{-1}) and explosion dates (± 7 days) reflects our uncertainties.

This expansion speed is much higher than the values reported in Brunthaler et al. (2009b). This discrepancy has three reasons: i) The lower value was based on a preliminary data reduction, without the data from the phased VLA and without the geodetic block corrections. ii) The radius of the brightest emission was used as an approximation for the source size. However, as shown here, this method underestimates the true expansion speed. iii) The sizes were measured by hand from the images and this gave an overestimated size in the first epoch, where the source was still very compact.

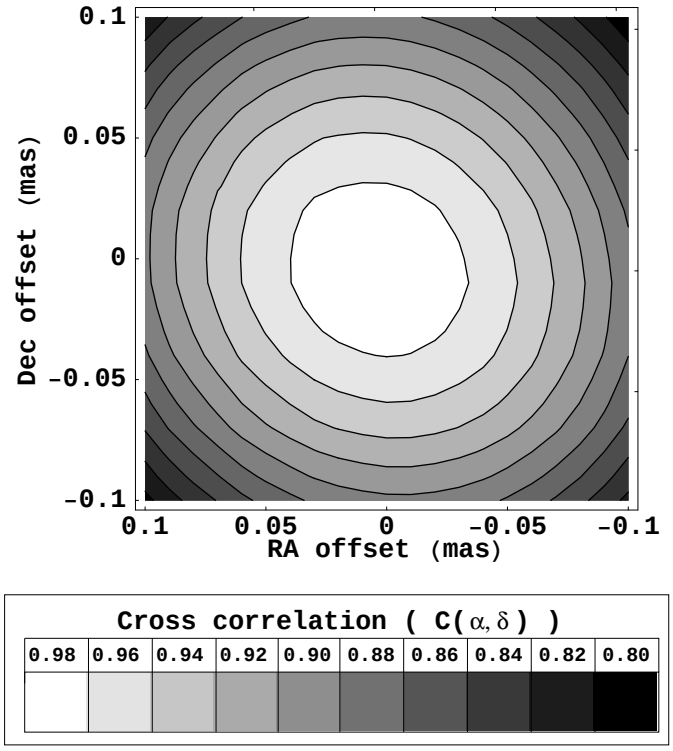

Fig. 7. Cross-correlation coefficient, $C(\alpha, \delta)$, between the images of the two VLBI epochs (scaling the first epoch to the size of the second), as a function of the coordinates of the explosion center, (α, δ), taking as reference the position of the maximum $C(\alpha, \delta)$ (see Sect. 4.3).

4.3. Expansion center, self-similarity, and anisotropic expansion

The ring is not symmetric and the brightest region in both images is the south-western part of the shell. This could be caused either by an asymmetry in the explosion or in the circumstellar medium (CSM), i.e. a clump with higher density in the southwest. A clumpy CSM is very common for red supergiant stars (e.g. Smith et al. 2009) which are likely progenitors for this supernova. Furthermore, a comparison of the 5 GHz light curve and the available 22 GHz data shows evidence for a clumpy CSM (Marchili et al. 2010).

As mentioned in section 4.1.1, we also estimated the central position of the ring. We do not detect any significant shift in the position, with an upper limit of ~ 50 μas in right ascension and 100 μas in declination. To verify the relative astrometric accuracy of the positions, we also imaged the three extragalactic background sources 0945+6924, 0948+6848, and 1004+6936. The average position change between the two observations of M81* relative to these quasars is 1±15 μas in right ascension and 22±53 μas in declination, where the uncertainties are the standard deviation[3]. Thus, we can rule out that any significant position shift is introduced by jet motion in M81*. We note that the angular separation of M82 to M81* is not larger than the angular separation between M81* and the three background quasars.

[3] These values give 1 σ upper limits on the proper motion of M81 of 260 km s^{-1} in right ascension and 1270 km s^{-1} in declination

Hence, systematic errors in the astrometry should be similar for all sources.

According to Chevalier (1982), the expansion of a supernova is self-similar, i.e., the source structure remains unaltered regardless of the source size. This model of a self-similar expansion has been extensively tested with SN 1993J (e.g. Marcaide et al. 1997, 2009a; Bartel et al. 2002). Although some deviations from self-similarity were found in the expansion of SN 1993J, this supernova kept its structure nearly self-similar during more than a decade. If the expansion of SN 2008iz was also self-similar between our two VLBI epochs, the VLBI images obtained should be equal (regardless of the global flux density scale) if we scale the first image to the size of the second one and use the same convolving beam for both images. However, the result of expanding the first VLBI image, to compare to the second one, depends on the point in the image that is chosen as the center of expansion. Therefore, a direct comparison between the images, to check the self-similarity in the expansion, is not possible if the coordinates of the expansion center of the supernova are not known.

To determine the coordinates of the expansion center of the supernova independently from the method described above, we computed different expanded versions of the image of the first VLBI epoch using different centers of expansion. The scaled images were obtained by scaling the positions of the CLEAN components of the model, according to the ratios of the supernova sizes reported in the previous section. We then used the same beam to convolve the CLEAN model of the second epoch and the resulting (scaled) CLEAN models of the first epoch. Finally, we compared the resulting image of the second epoch with the resulting (scaled) images of the first epoch by computing the cross correlation between both images using: we mean

$$C(\alpha,\delta) = \frac{\sum_i I_2^i \times I_1^i(\alpha,\delta)}{\sqrt{\sum_i \left(I_1^i(\alpha,\delta)\right)^2 \times \sum_i \left(I_2^i\right)^2}} \quad (2)$$

where I_2^i is the ith pixel of the image of the second epoch and $I_1^i(\alpha,\delta)$ is the ith pixel of the scaled version of the image of the first epoch, taking the point (α,δ) as the expansion center. Assuming a self-similar expansion, the coordinates of the maximum value of $C(\alpha,\delta)$ are an estimate of the position of expansion center of the supernova, which we identify as the coordinates of the explosion. In Fig. 7 we show the cross correlation of the images computed for different expansion centers, (α,δ), expanding the image of the first epoch according to the size estimated with the CPM. The maximum correlation (which corresponds to our estimate of the explosion center) takes place at the coordinates $\alpha = 09^{\rm h}\,55^{\rm m}\,51^{\rm s}.55025$ and $\delta = +69^\circ\,40'\,45''.79133$. These coordinates do not change by more than 10 μas if we use, instead, the size estimated with model-fitting to expand the image of the first VLBI epoch. This position agrees to the position given in Sect. 4.1.1 within 60 μas and verifies that the position of the expansion center has not changed between the two epochs.

Additionally, the value of $C(\alpha,\delta)$ at the maximum is a measure of the degree of self-similarity (and/or anisotropy) in the expansion. The maximum cross-correlation of the images is 0.98, if we use the CPM size to expand the image of the first epoch, and 0.97, if we use instead the model-fitting size. These values are very close to 1, which is the case of a perfect self-similar expansion. Therefore, we conclude that the expansion of SN 2008iz was self-similar to a high degree between our two VLBI epochs.

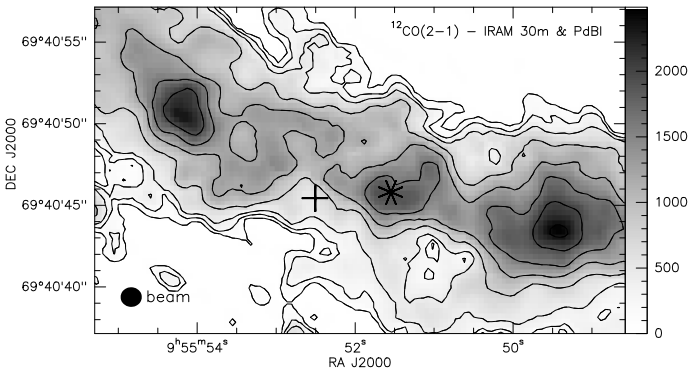

Fig. 8. ^{12}CO (J=2→1) intensity map of the central region of M82 from Weiß et al. (2001) with the positions of SN 2008iz (star) and the MERLIN transient (cross). The contours correspond to 200, 400, 600, 800, 1200 1600, 2000, and 2400 K kms^{-1}. The resolution of the observation is 1.5″ × 1.4″ (∼25 pc).

5. Discussion

5.1. Column density and extinction

The non-detection of SN 2008iz in the optical, infrared, and X-rays indicates that it exploded inside or behind a very dense cloud. Indeed, the ^{12}CO (J=2→1) line intensity map in Weiß et al. (2001) shows a prominent cloud exactly at the position of the supernova (Fig. 8). The line intensity at the position of SN 2008iz is ∼ 1800 K kms^{-1}. Using the Galactic conversion factor $X_{\rm CO} = 1.6 \times 10^{20}$ cm^{-2} (K kms^{-1})$^{-1}$, this corresponds to a H_2 column density $N(H_2)$ of $\sim 29 \times 10^{22}$ cm^{-2}. However, Weiß et al. (2001) find much smaller and spatially variable conversion factors from radiative transfer calculations, that lead to smaller H_2 column densities. At the position of SN 2008iz, the conversion factor is $\sim 0.3 \times 10^{20}$ cm^{-2} (K kms^{-1})$^{-1}$ (their Fig. 10). This leads to a H_2 column density of $\sim 5.4 \times 10^{22}$ cm^{-2}. However, the CO observations were performed with a linear resolution of ∼25 pc. Thus it is possible, that the supernova is located behind a smaller cloud with much higher column density. The ^{12}CO line intensity at the position of the MERLIN transient is almost 4 times smaller (∼500 K kms^{-1}).

Taking the latter value (5.4×10^{22} cm^{-2}) for N(H_2) and assuming that all of the column is between SN 2008iz and us, we derive a visual extinction, A_V, of 24.4 mag. Here we have used the relation between optical extinction and hydrogen nucleus column density, N(H), derived by Güver & Özel (2009) from X-ray absorption data of a sample of Galactic SNRs and assumed that all the hydrogen is in molecular form, i.e., N(H_2) = 2 N(H). Such a high value of the extinction would explain the lack of an optical counterpart.

The derived extinction is much higher than toward SN 1993J, for which Richmond et al. (1994) discuss values of $A_V = 0.7$ and 1.0 mag. With the extinction law given by Cardelli et al. (1989), $A_K = 0.114\,A_V$, we calculate 2.8 mag for the K−band (2.2 μm) extinction A_K. Fraser et al. (2009) report an even higher K-band extinction of up to 11 mag based on their non-detection (3σ upper limit on the absolute K-band magnitude of -5 mag) and the assumption that the infrared light curve of SN 2008iz behaves similar to the one of SN 1993J. Thus, SN 2008iz is either very weak in the infrared compared to SN 1993J, or behind a smaller but even denser cloud than estimated here.

Table 3. Comparison between SN 1993J and SN 2008iz.

Property		SN 1993J	SN 2008iz
spectral index α		-0.99[a]	-1.08[b]
L_{5GHz}	[10^{27}erg s^{-1} Hz^{-1}]	1.5[c]	2.5[d]
t_{peak}-t_0	[days]	180[c]	~120[d]
v_{VLBI}	[km s^{-1}]	14900[e]	21200[b]
$L_{X-ray\ at\ t\sim220\ days}$	[10^{38} erg s^{-1}]	~ 8[f]	< 15[b]

References: a) van Dyk et al. (1994); b) this work; c) Weiler et al. (1998); d) Marchili et al. (2010); e) Marcaide et al. (1995); f) Zimmermann & Aschenbach (2003).

5.2. Expansion velocity and synchrotron self-absorption

Chevalier (1998) proposed a way to estimate the mean expansion velocity of a supernova based on the radio-light curve and assuming that synchrotron self-absorption (SSA) dominates the light curve at the peak. If SSA is not the dominant absorption process at the peak of the light curve, then the estimate of the expansion velocity from the Chevalier (1998) model is a lower bound to the real expansion velocity of the radio shell. Following Chevalier (1998), the estimated mean expansion velocity at the peak of the radio-light curve, assuming dominant SSA, is:

$$V_{\rm SSA}({\rm km\,s^{-1}}) = 5.3786\times10^{6}(\beta\phi)^{-0.053}\left(\frac{F_{\rm p}}{1{\rm Jy}}\right)^{0.47}\times \left(\frac{D}{1{\rm Mpc}}\right)^{0.95}\left(\frac{\nu}{1.0\ {\rm GHz}}\right)^{-1}\left(\frac{t_p}{1{\rm day}}\right)^{-1} \quad (3)$$

where β is the ratio of the relativistic particle energy density to the magnetic field energy density (if we assume energy equipartition, $\beta = \frac{4}{3(1+k)}$, where k ranges from 1 to 2000, see Pacholczyk 1970, chapter 7), ϕ is the filling factor of the emitting region to a sphere (we assume a shell of width equal to 30% of the outer radius, which yields $\phi = 0.66$), $F_{\rm p}$ is the flux density at the peak, D is the distance, ν is the observing frequency, t_p is the supernova age at the peak, and we use a spectral index $\alpha = -1$ (see Eqs. 11 and 13 of Chevalier 1998).

For SN2008iz, Eq. 3 yields a mean expansion velocity (depending on k) in the range 8100 – 11800 km s^{-1} at the peak of the 5 GHz radio light curve. Using an expansion index of 0.89, these velocities translate into a mean expansion velocity in the range 7000 – 10300 km s^{-1} at the epoch of 27 April 2009. This range of velocities is a factor ~ 2 smaller than the velocities estimated from our VLBI observations, thus indicating that, in contrast to the case of SN1993J, SSA may not be an important absorption mechanism in the SN2008iz radio emission. This is also consistent with the results in Marchili et al. (2010) who were able to model the radio light curve of SN2008iz assuming that SSA effects are much smaller than free-free absorption (FFA) during the whole supernova expansion.

5.3. Comparison with other type II radio supernovae

Estimates of the expansion velocities of other type II radio supernovae have been estimated from VLBI observations, and very different results have been obtained. For instance, the mean expansion velocity of SN 1979C during the first year after explosion is estimated to be ~ 10000 – 11000 km s^{-1} (Bartel & Bietenholz 2003; Marcaide et al. 2009b); for SN 1986J, a velocity of ~ 14700 km s^{-1} was obtained by Pérez-Torres et al. (2002b), while Bietenholz et al. (2002) find 20000 km s^{-1} 3 month after the explosion; Staveley-Smith et al. (1993) report a mean expansion speed of ~ 35000 km s^{-1} during the first years for SN 1987A before it slowed down to ~ 4800 km s^{-1}; for SN 2004et, the expansion velocity was > 15700 km s^{-1} (Martí-Vidal et al. 2007); and for SN 2008ax, an expansion velocity as large as 52000 km s^{-1} was obtained (Martí-Vidal et al. 2009). Estimates of the expansion velocities of other supernova remnants in M82 (the host galaxy of SN 2008iz), have been also reported, which range between ~ 1500 and 11000 km s^{-1} (Beswick et al. 2006). These later velocities are much higher (a factor of 3 – 22) than the predicted velocities from the model of Chevalier & Fransson (2001), based on the high pressure expected in the interstellar medium (ISM) of M 82. The expansion velocity reported in this paper for SN2008iz is indeed a factor ~ 40 larger than the predicted velocities in Chevalier & Fransson (2001), although of the same order of magnitude than the velocities reported in Beswick et al. (2006) for the other remnants in M82, and the typical velocities of the other type II supernovae observed to date.

Weiler et al. (1998) find a correlation between peak radio luminosity at 5 GHz and the time between the explosion and the peak in the 5 GHz light curve for type II supernovae. The 5 GHz light curve of SN 2008iz from Marchili et al. (2010) gives a peak luminosity of ~ 2.5×10^{27}erg s^{-1} Hz^{-1} at ~120 days after the explosion. These values are well within the scatter of the correlation. Thus it seems plausible that SN 2008iz is also a type II supernova.

Since SN 2008iz and SN 1993J are located at very similar distances, this allows a detailed comparison between these two supernovae. Several properties of both supernovae are summarized in Table 3. The radio spectral indices, the peak radio luminosities, rise times, and early VLBI expansion velocities are similar (considering that the rise times and peak radio luminosities can vary by several orders of magnitudes for type II radio supernovae). The non-detection in X-rays of SN 2008iz can be attributed to absorption by the dense molecular cloud seen in the CO data.

6. Summary

In this paper we presented the first VLBI images, a VLA radio spectrum from 1.4 to 43 GHz, and Chandra X-ray observations of SN 2008iz. Our main results are:

- The VLBI images, separated by ~ 11 month show a shell-like structure expanding with a velocity of ~ 23000 km s^{-1}.
- The inferred expansion speed is a factor of 2 higher than expected if SSA dominates the light curve. This indicates that SSA is not important for the radio emission.
- The most likely explosion date is in mid February 2008, but not earlier than January 22 and not later than March 24.
- We find no evidence for an asymmetric explosion, but a high degree of self-similarity between the two VLBI observations.
- The VLA radio spectrum is well fitted by a broken power law with a turnover frequency of 1.5±0.1 GHz, and a spectral index of -1.08 ± 0.08 in the optically thin part.
- SN 2008iz is located behind (or inside) a large molecular cloud with a H_2 column density of 5.4×10^{22} cm^{-2} (on a scale of 25 pc), corresponding to a visual extinction, A_V, of 24.4 mag.
- Due to the high column density, we obtain only upper limits on the X-ray luminosity of 1.5×10^{41} and 1.5×10^{39}erg s^{-1} ~75 and ~200 days after the explosion, which is consistent

with the X-ray luminosity of SN 1993J at similar ages. We also obtain an upper limit for the X-ray luminosity of the second radio transient of 1.2×10^{38} erg s^{-1} (in 0.3–2.4 keV).

Acknowledgements. This work is partially based on observations with the 100-m telescope of the MPIfR (Max-Planck-Institut für Radioastronomie) at Effelsberg. MV is a fellow of the Alexander von Humboldt Foundation in Germany.

References

Bartel, N. & Bietenholz, M. F. 2003, ApJ, 591, 301
Bartel, N., Bietenholz, M. F., Rupen, M. P., et al. 2000, Science, 287, 112
Bartel, N., Bietenholz, M. F., Rupen, M. P., et al. 2002, ApJ, 581, 404
Bartel, N., Bietenholz, M. F., Rupen, M. P., & Dwarkadas, V. V. 2007, ApJ, 668, 924
Beswick, R. J., Muxlow, T. W. B., Pedlar, A., et al. 2009, The Astronomer's Telegram, 2060, 1
Beswick, R. J., Riley, J. D., Marti-Vidal, I., et al. 2006, MNRAS, 369, 1221
Bietenholz, M. F., Bartel, N., & Rupen, M. P. 2001, ApJ, 557, 770
Bietenholz, M. F., Bartel, N., & Rupen, M. P. 2002, ApJ, 581, 1132
Bietenholz, M. F., Bartel, N., & Rupen, M. P. 2003, ApJ, 597, 374
Brunthaler, A., Menten, K. M., Reid, M. J., et al. 2009a, A&A, 499, L17
Brunthaler, A., Menten, K. M., Reid, M. J., et al. 2009b, Central Bureau Electronic Telegrams, 1803, 1
Brunthaler, A., Reid, M. J., & Falcke, H. 2005, in ASP Conf. Ser. 340: Future Directions in High Resolution Astronomy, 455–+
Burrows, D. N., Hill, J. E., Nousek, J. A., et al. 2005, Space Science Reviews, 120, 165
Cappi, M., Palumbo, G. G. C., Pellegrini, S., & Persic, M. 1999, Astronomische Nachrichten, 320, 248
Cardelli, J. A., Clayton, G. C., & Mathis, J. S. 1989, ApJ, 345, 245
Chevalier, R. A. 1982, ApJ, 258, 790
Chevalier, R. A. 1998, ApJ, 499, 810
Chevalier, R. A. & Fransson, C. 2001, ApJ, 558, L27
Fox, D. W., Lewin, W. H. G., Fabian, A., et al. 2000, MNRAS, 319, 1154
Fraser, M., Smartt, S. J., Crockett, M., et al. 2009, The Astronomer's Telegram, 2131, 1
Freedman, W. L., Hughes, S. M., Madore, B. F., et al. 1994, ApJ, 427, 628
Gehrels, N., Chincarini, G., Giommi, P., et al. 2004, ApJ, 611, 1005
Güver, T. & Özel, F. 2009, MNRAS, 400, 2050
Marcaide, J. M., Alberdi, A., Ros, E., et al. 1995, Science, 270, 1475
Marcaide, J. M., Alberdi, A., Ros, E., et al. 1997, ApJ, 486, L31+
Marcaide, J. M., Martí-Vidal, I., Alberdi, A., et al. 2009a, A&A, 505, 927
Marcaide, J. M., Martí-Vidal, I., Perez-Torres, M. A., et al. 2009b, A&A, 503, 869
Marchili, N., Marti-Vidal, I., Brunthaler, A., et al. 2010, A&A, 509, A47
Martí-Vidal, I., Marcaide, J. M., Alberdi, A., et al. 2007, A&A, 470, 1071
Martí-Vidal, I., Marcaide, J. M., Alberdi, A., et al. 2009, A&A, 499, 649
Muxlow, T. W. B., Beswick, R. J., Garrington, S. T., et al. 2010, MNRAS, in press, arXiv:1003.0994
Muxlow, T. W. B., Beswick, R. J., Pedlar, A., et al. 2009, The Astronomer's Telegram, 2073, 1
Pacholczyk, A. G. 1970, Radio astrophysics. Nonthermal processes in galactic and extragalactic sources, ed. Pacholczyk, A. G.
Pérez-Torres, M. A., Alberdi, A., & Marcaide, J. M. 2001, A&A, 374, 997
Pérez-Torres, M. A., Alberdi, A., & Marcaide, J. M. 2002a, A&A, 394, 71
Pérez-Torres, M. A., Alberdi, A., Marcaide, J. M., et al. 2002b, MNRAS, 335, L23
Reid, M. J. & Brunthaler, A. 2004, ApJ, 616, 872
Richmond, M. W., Treffers, R. R., Filippenko, A. V., et al. 1994, AJ, 107, 1022
Shepherd, M. C., Pearson, T. J., & Taylor, G. B. 1995, in Bulletin of the American Astronomical Society, Vol. 27, Bulletin of the American Astronomical Society, ed. B. J. Butler & D. O. Muhleman, 903–+
Smith, N., Hinkle, K. H., & Ryde, N. 2009, AJ, 137, 3558
Staveley-Smith, L., Briggs, D. S., Rowe, A. C. H., et al. 1993, Nature, 366, 136
van Dyk, S. D., Weiler, K. W., Sramek, R. A., Rupen, M. P., & Panagia, N. 1994, ApJ, 432, L115
Weiler, K. W., Panagia, N., Montes, M. J., & Sramek, R. A. 2002, ARA&A, 40, 387
Weiler, K. W., van Dyk, S. D., Montes, M. J., Panagia, N., & Sramek, R. A. 1998, ApJ, 500, 51
Weiß, A., Neininger, N., Hüttemeister, S., & Klein, U. 2001, A&A, 365, 571
Zimmermann, H. & Aschenbach, B. 2003, A&A, 406, 969